

Stationary Propagation Characteristics for 5 GHz Wireless LAN Applications

Valentine J. Rhodes and Eric A. Jacobsen, *Member, IEEE*

Abstract—Empirical propagation characteristics of typical wireless LAN channels in the 5 GHz to 6 GHz spectrum are presented in this paper. A network analyzer was used to measure the stationary channel frequency response and an inverse Fourier transform was used to obtain the channel impulse response. Measurements were taken in four residential settings and one office/cubicle setting. Path loss and delay spread results are presented according to the measurement environment: residential, office, indoor-indoor, indoor-outdoor, and the number of walls penetrated. This categorization of measurement data lends itself to several new conclusions: non-line-of sight (NLOS) path loss exponents are similar to line-of-sight (LOS) exponents with an additional wall attenuation factor, delay spread increases with each wall penetrated, delay spread increases when the receiver is placed outdoors, delay spread is greater in a cubicle environment than a residential environment, and the IEEE 802.11 delay spread model shows close agreement with the measured data. Given these findings, a new simplified channel model is proposed for simulating the static propagation behavior in this band and these environments.

Index Terms—Channel model, path loss, delay spread, wireless LAN.

I. INTRODUCTION

The use of wireless LAN (WLAN) equipment and the recent introduction of products in the 5 GHz to 6 GHz band suggest that proliferation of devices in this spectrum will see an increasing trend. In order to design new WLAN systems, the wireless channels for the target environment must be better understood. Similar to other related unlicensed bands (e.g. 2.4 GHz) for which propagation behaviors have been heavily

characterized, wireless channel propagation studies in the 5 GHz to 6 GHz region [1]-[5] have only recently become the subject of attention. This paper complements previous work and further identifies environmental classifications to obtain simple, yet accurate, propagation characteristics for a given channel scenario.

Full characterization of anticipated WLAN environments is difficult given the variety of possible practical scenarios. The sizes and shapes of buildings, construction materials, placement and materials of furnishings, arrangements of interior walls, and quantity and placement of windows, all affect the multi-path reflections and losses in each channel. Channels found in residential environments can be expected to differ from those found in office environments due to cubicle walls, suspended ceilings, and metal file cabinets. Furthermore, indoor-to-indoor channels can be expected to differ from indoor-to-outdoor channels due to the greater multi-path propagation distances and the difference in penetrating an external wall versus interior walls only. The large number of environmental variations drove further investigation into not only empirical propagation characterization, but in classifying the different types of environmental factors for appropriate model generation. Additional characteristics such as penetration losses per indoor wall and cross-polarization effects were analyzed as well. The results of these analyses allow us to present a new, simple path loss model and important additions to the IEEE 802.11 delay spread model.

The path loss and delay spread profiles covered in this paper were examined for a variety of conditions to determine those parameters that had the greatest statistical impact on the channel classifications. After extensive analysis of the data, it was determined that the channels were best classified by residential indoor-to-indoor, office indoor-to-indoor, and residential indoor-to-outdoor.

II. EQUIPMENT, METHODOLOGY, AND SITE DESCRIPTIONS

A Vector Network Analyzer (VNA) was used to measure the channel frequency response [1], [6]-[12]. Fig. 1 shows a block diagram of the data collection system. An Agilent 8753ET Transmission/Reflection

Network Analyzer was used to provide the stimulus and measure the response. The transmit (Tx) and receive (Rx) antennas were omni-directional quarter-wave length monopoles with center frequencies of 5.250 GHz. A purpose-built receiver was used which drove 100 feet of LMR-400 coaxial return cable. For all links tested, the spectrum from 5 to 6 GHz was sampled by the VNA in the frequency domain. Frequency samples measuring the magnitude and phase response of the channel were made with 1601 samples taken across the band with a resolution bandwidth of 3.7 kHz. This provided frequency sample spacing of 625 kHz. In all cases, the response of the cables and receiver electronics were calibrated out by the VNA. The worst case noise floor was set to -30 dBc and was generally better. Ten measurements were recorded, and averaged, thus dropping the noise floor to 40 dB below the signal power.

Using the equipment shown in Fig. 1, point-to-point single-input-single-output (SISO) channels were measured in four residential settings as well as a cubicle office environment. Multiple channels were measured in each location from likely access point locations to diverse likely terminal locations. The five sites used are described as follows:

1. Site R1 - Single story residential. Stucco on 2x6 construction exterior walls and paper-faced fiberglass insulation. Occupied with typical furnishings throughout the house. Four different transmitter locations and thirty-three receiver locations were tested, with eleven of those outdoor. A total of 128 links were tested at this site.
2. Site R2 - Two story residential. Wood construction with stucco exterior walls. Two transmitter locations and twenty-five receiver locations were tested with six outdoor. One of the transmitter and nine of the receiver locations were on the second floor. A total of 50 links were tested at this site.
3. Site R3 - Second floor walk-up condominium. Wood construction with stucco exterior walls. Unoccupied with no furnishings. Two transmitter locations and twenty-six receiver locations were tested with seven of these being outdoor. Five of the indoor-to-outdoor links were from the second floor to ground level. A total of 47 links were tested at this site.

4. Site R4 - Single story residential with open loft. Block construction with stucco and brick exterior finish. Occupied with typical furnishings throughout the house. Two transmitter locations and twenty three receiver locations were tested with five of these being outdoor. One of the transmitter and two of the receiver locations were on the second floor loft. A total of 46 links were tested at this site.

5. Site O1 - Single floor office area. This is a typical large office environment with large open areas occupied by cubicle (soft partition walls) office furniture and enclosed conference rooms. Two areas were tested: an office cubicle area with adjacent conference rooms, and a cafeteria/break area with an outdoor courtyard. In the cubicle area, two transmitter locations and twenty-two receiver locations were tested with two in enclosed conference rooms. The two transmitter locations differed only in antenna height with one at desk level and one at ceiling level. In the cafeteria area, one transmitter location and ten receiver locations were tested with three of those in the outdoor courtyard. All ten links in the cafeteria were tested with the antennas in both co-polarization and cross-polarization configuration. A total of 64 links were tested at this site.

All residential sites were of wood frame construction with gypsum wallboard covering interior walls and block walls at the property line. The office building is of block construction with typical cubicle furniture and interior walls of gypsum wallboard on metal studs.

For all of the residential and office/cubicle tests, the antennas were co-polarized vertically. In the office cafeteria, both vertical co-polarization and cross polarization tests were performed for each link with the transmit antenna being horizontally polarized for the cross-polarization experiments. In all of the residential cases and the office cafeteria case, both indoor-to-indoor and indoor-to-outdoor links were tested.

A number of parameters were recorded for each link tested including site and locations of the transmitter and receiver, the range, i.e., the distance between the transmitter and receiver, the relative heights of the

antennas, the number of walls penetrated, and the setting of the step attenuator in the receiver which was adjusted for each link to manage the limited dynamic range of the test equipment.

III. PATH LOSS

The VNA records the relative magnitude and phase of the received sinusoid with respect to a transmitted sinusoid for each of the 1601 frequencies across the 5-6 GHz band. By inverting the relative power, the attenuation, or path loss, is obtained for that Tx-Rx antenna separation. The theoretical path loss in dB as a function of distance [1], [2], [13] is given by

$$PL(d) = 20 \log\left(\frac{4\pi d_0}{\lambda}\right) + 10n \log\left(\frac{d}{d_0}\right) \quad (1)$$

where λ is the center frequency wavelength (5.5 GHz in this case), $d_0=1$ meter is the free space reference distance from the transmitter, n is the path loss exponent, and d is the distance between the antennas. An additional attenuation term A_0 has been added to the theoretical path loss

$$PL(d) = 20 \log\left(\frac{4\pi d_0}{\lambda}\right) + 10n \log\left(\frac{d}{d_0}\right) + A_0 \quad (2)$$

to compensate for the gain due to multi-path addition, wall attenuation, and antenna gain. This is similar to the Wall Attenuation Factor (WAF) and Floor Attenuation Factor (FAF) models [14]-[15] developed for path loss prediction of cellular band frequencies at 900 MHz. In general, A_0 is frequency dependent but is shown here as a constant for the average frequency of 5.5 GHz as measured. Following analysis of the collected data, the frequency dependence of the attenuation was found to be negligible when compared to the multi-path effects. This allowed the data to be separated into ten 100 MHz bands, consistent with the majority of world-wide 5 GHz spectrum as proposed by the International Telecommunications Union Radio Communications Sector (ITU-R).

The path loss plots for various channel classifications (residential indoor-to-indoor, office indoor-to-indoor, residential indoor-to-outdoor, LOS, and number of walls penetrated) are shown in Fig. 2a-c. The

points shown in Fig. 2 correspond to the measured path loss for each of the ten 100 MHz bands. Since site R4 consisted of different exterior wall construction than sites R1 through R3, the indoor-to-outdoor data corresponding to R4 was removed in order to obtain more accurate curves for similar construction types as shown in Fig. 2d. All path loss results presented in this paper were calculated with the outdoor measurements of R4 removed. For each of the environments shown in Fig. 2a-b,d, the values for n , A_0 , and the standard deviation, σ , corresponding to (2) are given in Table 1. For most NLOS environments, measurements were not available at 1 meter so a least squares log linear extrapolation was used to determine the intercept point used to determine A_0 .

Path loss exponents less than $n=2$ for LOS channels and greater than $n=2$ for NLOS channels have been independently reported [17], [22]-[23]. The NLOS path loss exponents presented in this paper appear to contradict the previously published findings. Since the presented path loss curves are grouped according to number of walls penetrated, the path loss exponent is similar to LOS with an additional wall attenuation factor accounted for in A_0 . For comparison, without explicitly grouping by walls penetrated, the residential 1 meter attenuation factor, A_0 , and path loss exponent, n , were found to be -3.14 and 3.19 respectively, similar to previously published results.

Additional observations were made from the collected data. The attenuation per interior office wall was found to match that of the interior residential walls. Approximately 4.5 dB of attenuation was observed per interior wall, ceiling/floor pair, and 9 dB of attenuation per exterior wall. Approximately 6 dB of loss was observed due to cross polarization of the Tx and Rx antennas. Mounting the Tx antenna on the suspended ceiling of the office environment at a height of 2.77 meters made no difference to the average path loss profiles when compared to the desktop height case. In some cases, a Tx ceiling mount provided a LOS channel and therefore additional power gain, but in other cases, the desk mount provided a channel obstructed only by soft partition walls whereas the ceiling mount introduced raised metal book cases into the channel. The soft partition wall attenuation was found to be much less than the attenuation of the

residential walls. On average, the cubicle wall separation was 2.5 meters. Without accounting for each soft wall attenuation, the NLOS path loss exponent was found to be greater than LOS. Antenna angles were varied in the measurement environments with no affect on the measured frequency response, implying that multi-path effects dominated any non-ideal antenna pattern effects.

IV. DELAY SPREAD

To calculate the delay spread statistics, each 100 MHz band was isolated, shifted to base band, and normalized to unit power. A Hamming window was applied to the base band samples, zero-padded from 161 to 512 samples, and an inverse Fourier transform was used to obtain the impulse response. The samples below the first side-lobe of the Hamming window at -43 dB were set to zero so as not to bias the delay spread result. The peak of the first impulse was shifted to time zero and the power was re-normalized to unity. Impulse response sets, corresponding to various parametric groupings (environment, number of walls penetrated, frequency band) were averaged to obtain a resultant delay spread profile. The mean (excess) and the root mean square (rms) delay spread values were calculated using (3) and (4) respectively, where p_n is the sampled power profile, t_n is the sampling time, and P_T is its total power [16].

$$\tau_{\mu} = \frac{1}{P_T} \sum_{n=0}^{N-1} p_n t_n \quad (3)$$

$$\tau_{\text{rms}} = \sqrt{\frac{1}{P_T} \sum_{n=0}^{N-1} p_n t_n^2 - \tau_{\mu}^2} \quad (4)$$

The use of a window prior to the Fourier transform has been reported to increase the delay spread estimate [17]-[18]. This was found to be algorithm dependent. If the side lobe samples were not set to zero, the estimate using a rectangular window is larger than the Hamming window due to the large side lobe power of the rectangular window. If the side lobe levels were set to zero, the use of a window increased not only the main lobe width, but also allowed the energy from longer multi-path signals (i.e. lower power) to

influence the estimate. This algorithm resulted in a consistent and accurate fit of the collected data with the established 802.11 channel model.

The delay spread profiles for the various environment classifications are shown in Fig. 3 and the corresponding delay spread parameters are shown in Table II. The legend in Fig. 3 denotes residential/office environment, indoor/outdoor location of the receiver, and the number of walls between the antennas. The shortest delay was observed with LOS channels in the residential environment and the longest delay spread was observed with NLOS channels in the office environment.

V. MEASURED VS. 802.11 DELAY SPREAD MODEL

The 802.11 exponential delay spread model [19]-[21] is repeated here for convenience. The channel is modeled by a Finite Impulse Response (FIR) filter where the taps are independent complex Gaussian random variables with zero mean and average power σ_k^2 ,

$$h_k = \mathcal{N}\left(0, \frac{1}{2}\sigma_k^2\right) + j\mathcal{N}\left(0, \frac{1}{2}\sigma_k^2\right) \quad (5)$$

for

$$k = 0, 1, \dots, k_{\max} \quad (6)$$

$$k_{\max} = \frac{10\tau_{\text{rms}}}{T_s} \quad (7)$$

$$\beta = e^{-T_s/\tau_{\text{rms}}} \quad (8)$$

$$\sigma_0^2 = \frac{1-\beta}{1-\beta^{k_{\max}+1}} \quad (9)$$

$$\sigma_k^2 = \sigma_0^2\beta^k \quad (10)$$

where τ_{rms} is the rms delay spread and T_s is the sampling period.

The measured delay spread profiles from Fig. 3 are compared to the 802.11 delay spread model in Fig. 4 for the two shortest delay spread environments and the two longest delay spread environments. Although

not shown here, all measured delay spread profiles agree with the 802.11 model. As expected from the Central Limit Theorem, the complex impulse response samples were found to have a Gaussian distribution.

VI. CHANNEL MODEL FIT TO EMPIRICAL MEASUREMENTS

The path loss and delay spread empirical results may be simplified to a general fit for the 5 GHz wireless LAN channels as measured. The result of simplifying the path loss curves is shown in Fig. 5 where the solid curves were derived from the measured data and the dashed lines correspond to Fig. 2a-b,d. The legend in Fig. 5 reflects only the model curves. The path loss and delay spread parameters for this model are given in Table III where N_w is the number of walls penetrated. The use of Table III in conjunction with (2) and (5)-(10) offer a simple channel model based on measured data in the 5-6 GHz band. It should be noted that little data was available for the three-wall scenario. Therefore, the three-wall conclusions were drawn from the two-wall and four-wall measurements.

VII. CONCLUSIONS

Propagation measurements in the 5 GHz to 6 GHz band were made in residential and office environments thought to encompass a majority of WLAN deployment settings. Analysis of channel measurements led to a simplified static channel model for use in WLAN system and simulation design. The key result of this work is that once key attenuation factors, walls in this case, are known, an LOS path loss exponent may be used in conjunction with step attenuation parameters to predict the path loss characterization for the given placement of WLAN equipment. This work also suggests that the delay spread for equipment placement may be predicted. Although the measurement environments were chosen due to the typical nature of their construction, they represent only a small subset of construction styles and materials. This suggests that future measurements with varying construction types would be relevant work in this area, adding to the channel model presented here.

ACKNOWLEDGEMENT

We wish to thank Bud Nation, Cliff Prettie, and David Cheung for their unrelenting scrutiny of the results and their support throughout this effort.

REFERENCES

- [1] Kumar, S.P.T.; Farhang-Boroujeny, B.; Uysal, S.; Ng, C.S., "Microwave indoor radio propagation measurements and modeling at 5 GHz for future wireless LAN systems," *Microwave Conference, 1999*, vol. 3, pp. 606-609, 1999.
- [2] Mangold, S.; Lott, M.; Evans, D.; Fifield, R., "Indoor radio channel modeling-bridging from propagation details to simulation," *Personal Indoor and Mobile Radio Communications, The Ninth IEEE International Symposium on*, Vol. 2, pp. 625-629, 1998.
- [3] Xiongwen Zhao; Kivinen, J.; Vainnikainen, P., "Tapped delay line channel models at 5.3 GHz in indoor environments," *Vehicular Technology Conference, 2000*, Vol. 1, pp. 1-5, 2000.
- [4] Kivinen, J.; Xiongwen Zhao; Vainikainen, P., "Empirical characterization of wideband indoor radio channel at 5.3 GHz," *Antennas and Propagation, IEEE Transactions on*, Vol. 49, Issue 8, pp. 1192-1203, Aug. 2001.
- [5] Cuinas, I.; Sanchez, M.G., "Measuring, modeling, and characterizing of indoor radio channel at 5.8 GHz," *Vehicular Technology, IEEE Transactions on* , Vol. 50, Issue 2, pp. 526-535, March 2001.
- [6] Santella, G.; Restuccia, E., "Analysis of frequency domain wide-band measurements of the indoor radio channel at 1, 5.5, 10 and 18 GHz," *Global Telecommunications Conference, 1996. GLOBECOM '96. Communications: The Key to Global Prosperity*, Vol. 2, pp. 1162-1166, 1996.

- [7] Babich, F.; Lombardi, G.; Tomasi, L.; Valentinuzzi, E., "Indoor propagation measurements at DECT frequencies," *Electrotechnical Conference, 1996. MELECON '96, 8th Mediterranean*, Vol. 3, pp. 1355-1359, 1996.
- [8] Hashemi, H., "Impulse response modeling of indoor radio propagation channels," *Selected Areas in Communications, IEEE Journal on*, Vol. 11, Issue 7, pp. 967-978, Sept. 1993.
- [9] Zaharia, G.; El Zein, G.; Citerne, J., "Time delay measurements in the frequency domain for indoor radio propagation," *Antennas and Propagation Society International Symposium*, Vol. 3, pp. 1388-1391, 1992.
- [10] Janssen, G.J.M.; Prasad, R., "Propagation measurements in an indoor radio environment at 2.4 GHz, 4.75 GHz and 11.5 GHz," *Vehicular Technology Conference, 1992, IEEE 42nd*, Vol. 2, pp. 617-620, 1992.
- [11] Zaghoul, H.; Morrison, G.; Fattouche, M., "Frequency response and path loss measurements of indoor channel," *Electronics Letters*, Vol. 27, Issue 12, pp. 1021-1022, 1991.
- [12] Howard, S.J.; Pahlavan, K., "Measurement and analysis of the indoor radio channel in the frequency domain," *Instrumentation and Measurement, IEEE Transactions on*, Vol. 39, Issue 5, pp. 751-755, 1990.
- [13] Freeman, Roger L., *Radio System Design for Telecommunications*. John Wiley & Sons, 1997.
- [14] Rapport, T., *Wireless Communication: Principles and Practice*, Prentice Hall, 2002.
- [15] Seidel, S., "914 MHz Path Loss Prediction Models for Indoor Wireless Communications in Multifloored Buildings," *IEEE Trans. On Antennas and Propagation*, Vol. 40, No. 2, Feb. 1992.
- [16] Saunders, Simon R., *Antennas and Propagation for Wireless Communication Systems*, John Wiley & Sons, 1999.
- [17] Rusch, Leslie, Prettie, Cliff, Cheung, David, Li, Qinghua, Ho, Minnie, "UWB Channel Measurements for the Home Environment," *UWB Intel Forum*, Portland, OR, Oct. 2001.
- [18] Howard, Steven J., Pahlavan, Kaveh, "Autoregressive Modeling of Wide-Band Indoor Radio Propagation," *Communcations, IEEE Transactions on*, Vol. 40, No. 9, pp. 1540-1552, Sept. 1992.

- [19] Chayat, Naftali, “Tentative Criteria for Comparison of Modulation Methods,” doc.: IEEE 802.11-97/96. Sept. 1997.
- [20] Chatay, Naftali, “Updated Submission Template for TGa – revision 2,” doc.: IEEE 802.11-98/156r2, March 1998.
- [21] Halford, Steve, Halford, Karen, Webster, Mark, “Evaluating the Performance of HRb Proposals in the Presence of Multipath,” doc.: IEEE 802.11-00/282r2, Sept. 2000.
- [22] Ghassemzadeh, S., “Characterization of Ultra-Wide Bandwidth Channel at 5 GHz,” *Intel UWB Forum*, Portland, OR, Oct. 2001.
- [23] Ghassemzadeh, S., Jana, R., Rice, C., Turin, W., Tarokh, V., “A Statistical Path Loss Model for In-Home UWB Channels,” *Ultra Wideband Systems and Technologies, 2002 IEEE Conference on*, pp. 59-64.

Valentine J. Rhodes received his BSEE in 1985 from the University of Arizona, Tucson, AZ and his MSEE in 1990 from Arizona State University, Tempe, AZ.

He has held engineering research and development positions at Honeywell, Orbital Sciences, California Microwave/EFData, and Sicom. Previous research topics include adaptive noise cancellation and digital demodulation algorithms for satellite modem applications. He is currently employed with Intel Corporation, Chandler, AZ, where his research topics include physical layer OFDM algorithms for IEEE 802.16 and IEEE 802.11 applications.

Eric A. Jacobsen (M’83) obtained BSEE and MSEE degrees from the South Dakota School of Mines and Technology in 1985 and 1990, respectively.

He has held research and advanced development positions at Goodyear Aerospace, Honeywell, and California Microwave/EFData. He is currently investigating advanced algorithms and techniques for high speed wireless LAN systems with Intel in Chandler, AZ, where he leads the Advanced OFDM research efforts within Intel Labs. His research interests have included radar and image processing, passive acoustic

tracking, avionics, and efficient signal processing and coding for satellite communication systems. His latest interests include efficient OFDM modulation and coding techniques, smart antennas, adaptation methods, and multiple access schemes.

Mr. Jacobsen is a member of Eta Kappa Nu and Tau Beta Pi and has contributed as a member of the IEEE 802.16 and 802.11 standard working groups.

TABLES AND FIGURES

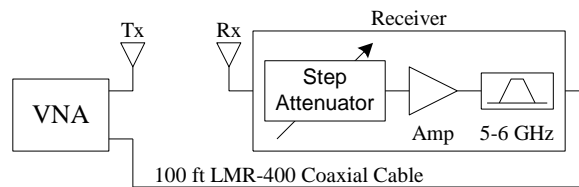
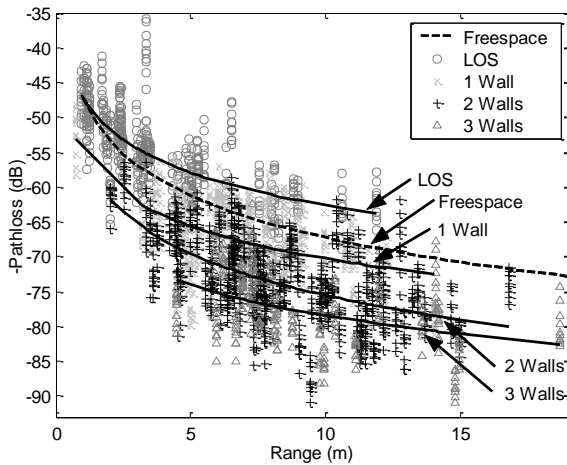
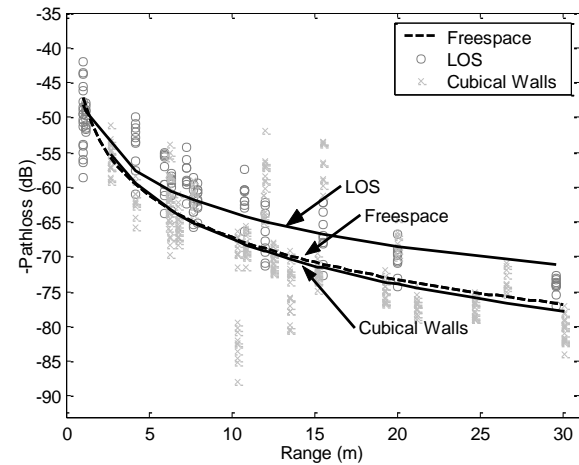


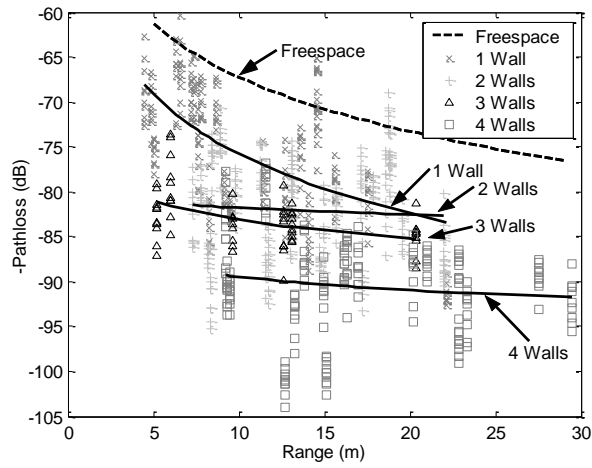
Fig. 1 Data collection equipment diagram.



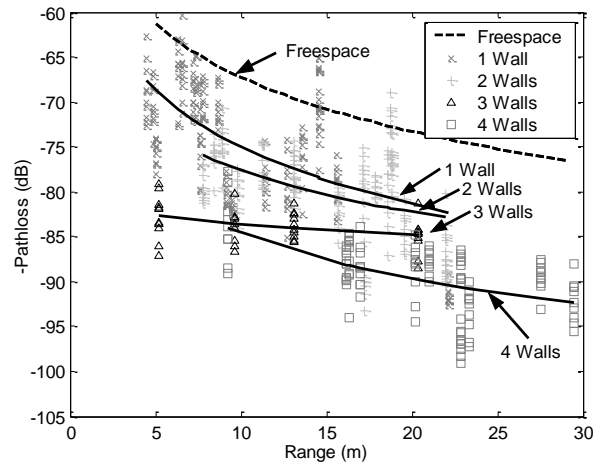
(a) Residential indoor



(b) Office indoor



(c) Residential outdoor – all sites



(d) Residential outdoor – R4 removed

Fig. 2 Path loss vs. range for residential and office sites.

Table 1 - 1 Meter Attenuation and Exponent Values

Environment	A_0 (dB)	n	σ (dB)
Freespace	0	2	
Residential Indoor (Fig. 2a)			
LOS	-0.19	1.56	4.22
1 Wall	7.70	1.53	5.12
2 Walls	8.38	1.99	5.00
3 Walls	16.27	1.50	4.82
Residential Outdoor All Sites (Fig. 2b)			
1 Wall	6.39	2.21	5.77
2 Walls	32.13	0.24	5.44
3 Walls	28.71	0.71	2.79

4 Walls	37.27	0.49	5.34
Residential Outdoor R4 Removed (Fig. 2c)			
1 Wall	6.54	2.12	5.56
2 Walls	15.07	1.53	4.53
3 Walls	32.82	0.36	2.02
4 Walls	21.01	1.64	3.25
Office Indoor (Fig. 2d)			
LOS	0.50	1.59	3.51
NLOS	-1.27	2.15	5.31
Residential Indoor NLOS	-3.14	3.19	2.62
(all measurements)			

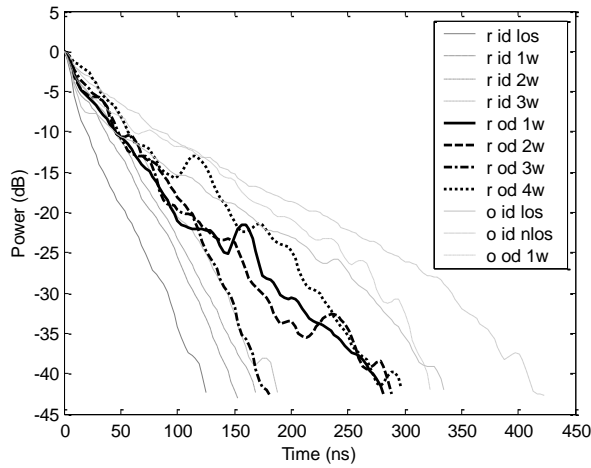
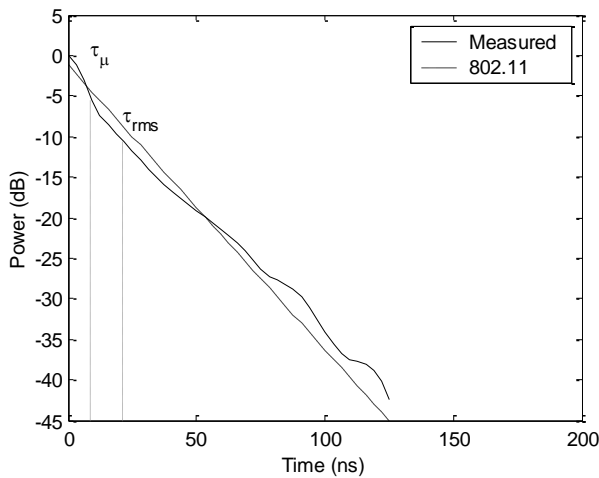
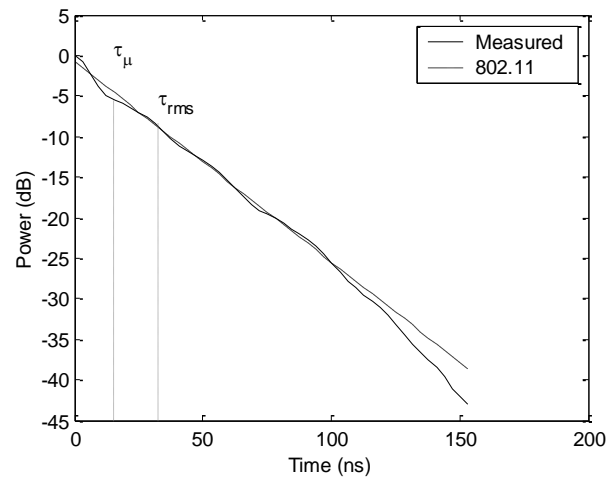


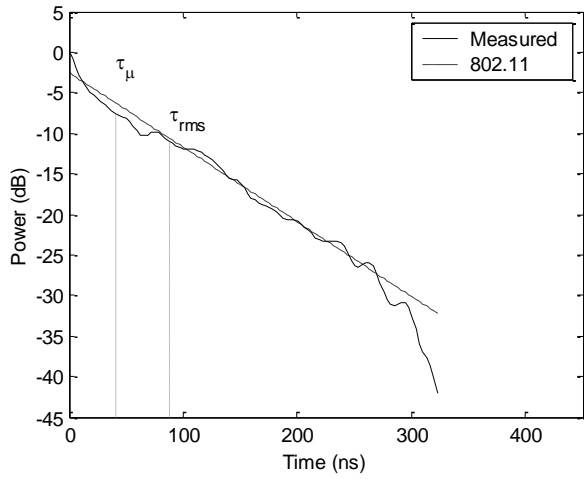
Fig. 3 Delay spread comparison.



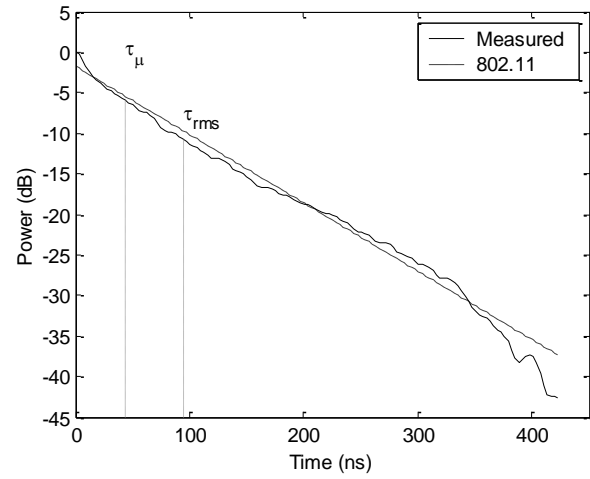
(a) Residential indoor LOS (r id los)



(b) Residential indoor 1 wall (r id 1w)



(c) Office outdoor 1 wall (o od 1w)



(d) Office indoor NLOS (o id nlos)

Fig. 4 Measured vs. 802.11 delay spread

Table II – Mean, RMS, and -43 dB Delay Spread

Environment	τ_{μ} (ns)	τ_{rms} (ns)	$\tau_{-43\text{dB}}$ (ns)
Residential Indoor			
LOS (r id los)	9	12	125
1 Wall (r id 1)	15	18	153
2 Walls (r id 2)	18	19	169
3 Walls (r id 3)	22	21	188
Residential Outdoor			
1 Wall (r od 1)	22	28	282
2 Walls (r od 2)	24	28	288
3 Walls (r od 3)	21	22	182
4 Walls (r od 4)	29	33	297

Office Indoor			
LOS (o id los)	33	44	335
NLOS(o id nlos)	44	52	423
Office Outdoor			
1 Wall (o od 1)	41	47	323

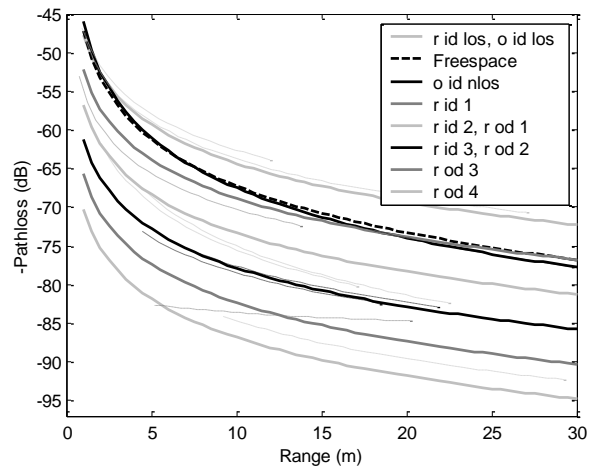


Fig. 5 Channel model path loss curves.

Table III – Channel Model Parameters

Environment	A_0	n	τ_{rms} (ns)
Residential Indoor	$0.5 + 4.5N_w$	1.66	$12 + 3N_w$
Residential Outdoor	$0.5 + 4.5(N_w + 1)$	1.66	$26.33 + 1.67N_w$
Office Indoor			
LOS	$0.5 + 4.5N_w$	1.66	$44 + 3N_w$
NLOS	-1.25	2.15	52
Office Outdoor	$1.25 + 4.5(N_w + 1)$	2.15	$44 + 3N_w$